Supplementary Information for

MODIS Collection 6.1 aerosol optical depth products over land and ocean: validation and comparison

Jing Wei[1], Zhanqing Li[1,2]*, Yiran Peng[3], Lin Sun[4]

[1. State Key Laboratory of Remote Sensing Science, Beijing Normal University, Beijing, China; 2. Department of Atmospheric and Oceanic Science, Earth System Science Interdisciplinary Center, University of Maryland, College Park, MD, USA; 3. Ministry of Education Key Laboratory for Earth System Modeling, Department of Earth System Science, Tsinghua University, Beijing, China; 4. College of Geomatics, Shandong University of Science and Technology, Qingdao, China]
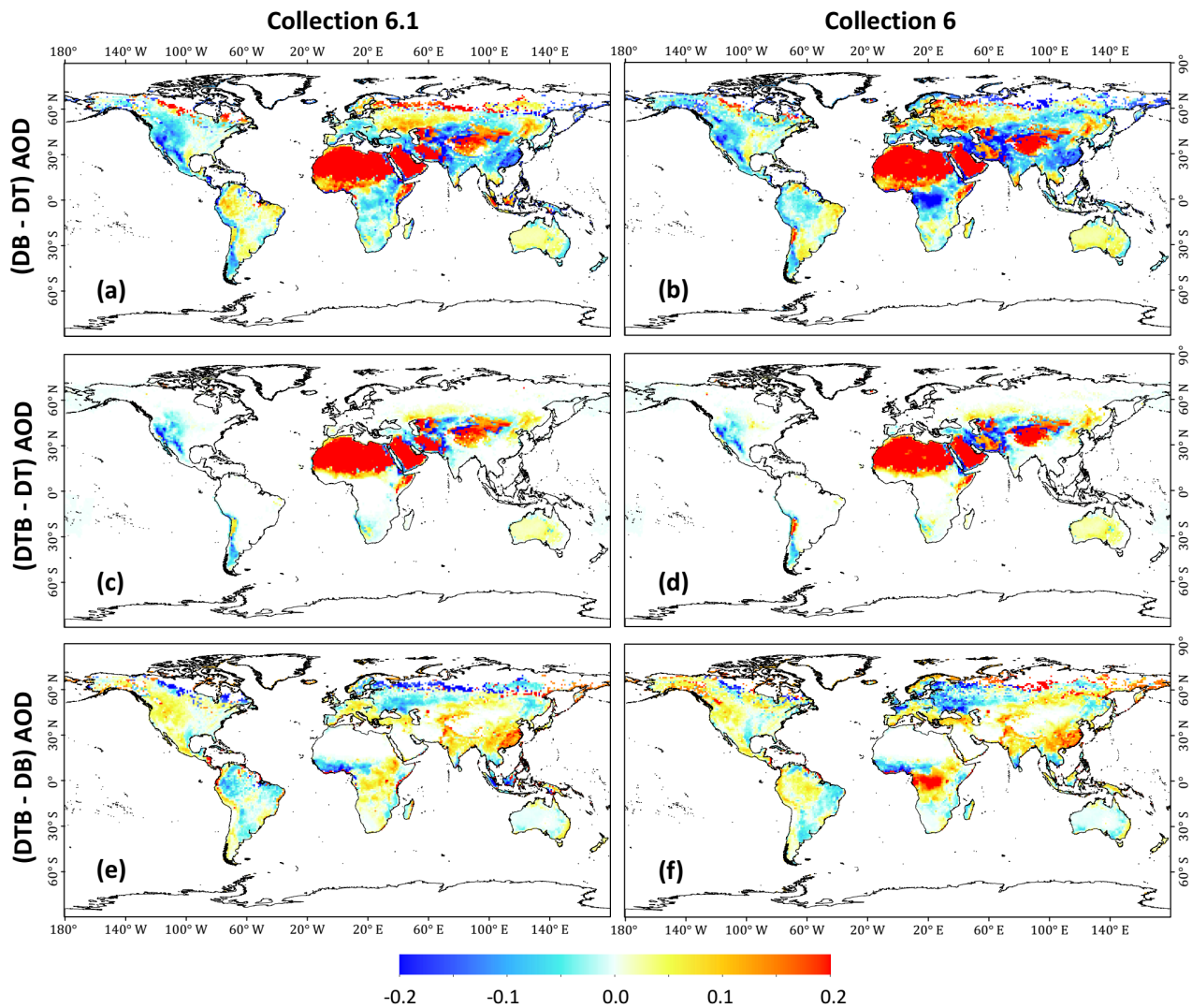
Contents of this file

Figure S1. Mean differences in C6.1 (left panels) and C6 (right panels) annual mean AODs between (a, b) DB and DT, (c, d) DTB and DT, and (e, f) DTB and DT. Data are from 2013–2017.
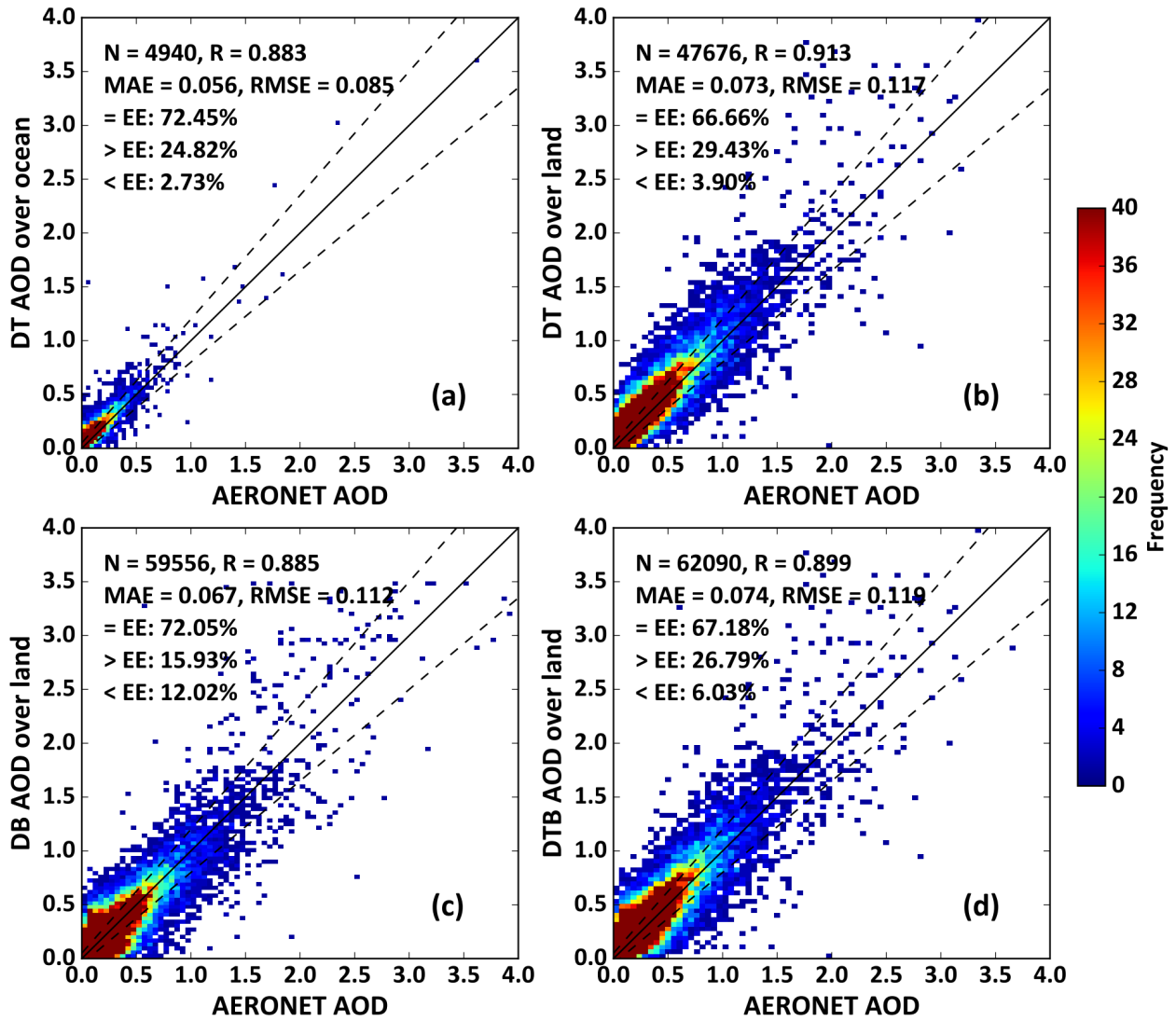
Figure S2. Density scatter plots of Terra MODIS C6 DT over ocean (a), DT (b), DB (c) and DTB (c) AOD retrievals over land against AERONET AOD measurements from 2013 to 2017. The solid line denotes the 1:1 line, and the dashed lines denote the envelope of the expected error (EE). The sample size (N), correlation coefficient (R), mean absolute error (MAE), and root-mean-square error (RMSE) are also given.
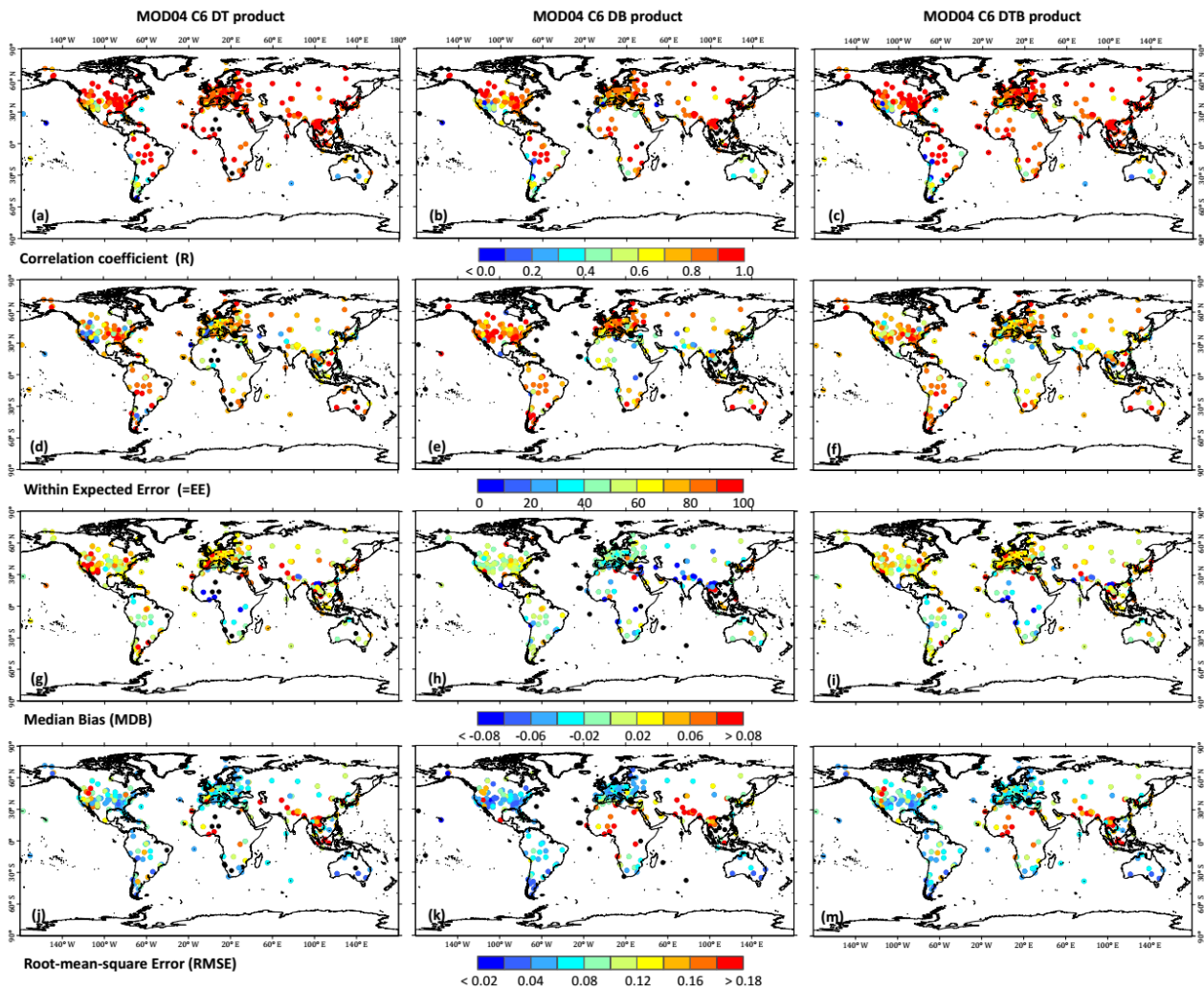
Figure S3. Validation of Terra MODIS C6 DT, DB, and DTB AOD retrievals against AERONET AODs for each site from 2003 to 2017: (a-c) correlation (R), (d-f) percentage of retrievals winthin the expected error envelope (%), (g-i) median bias, and (j-m) root-mean-square error.
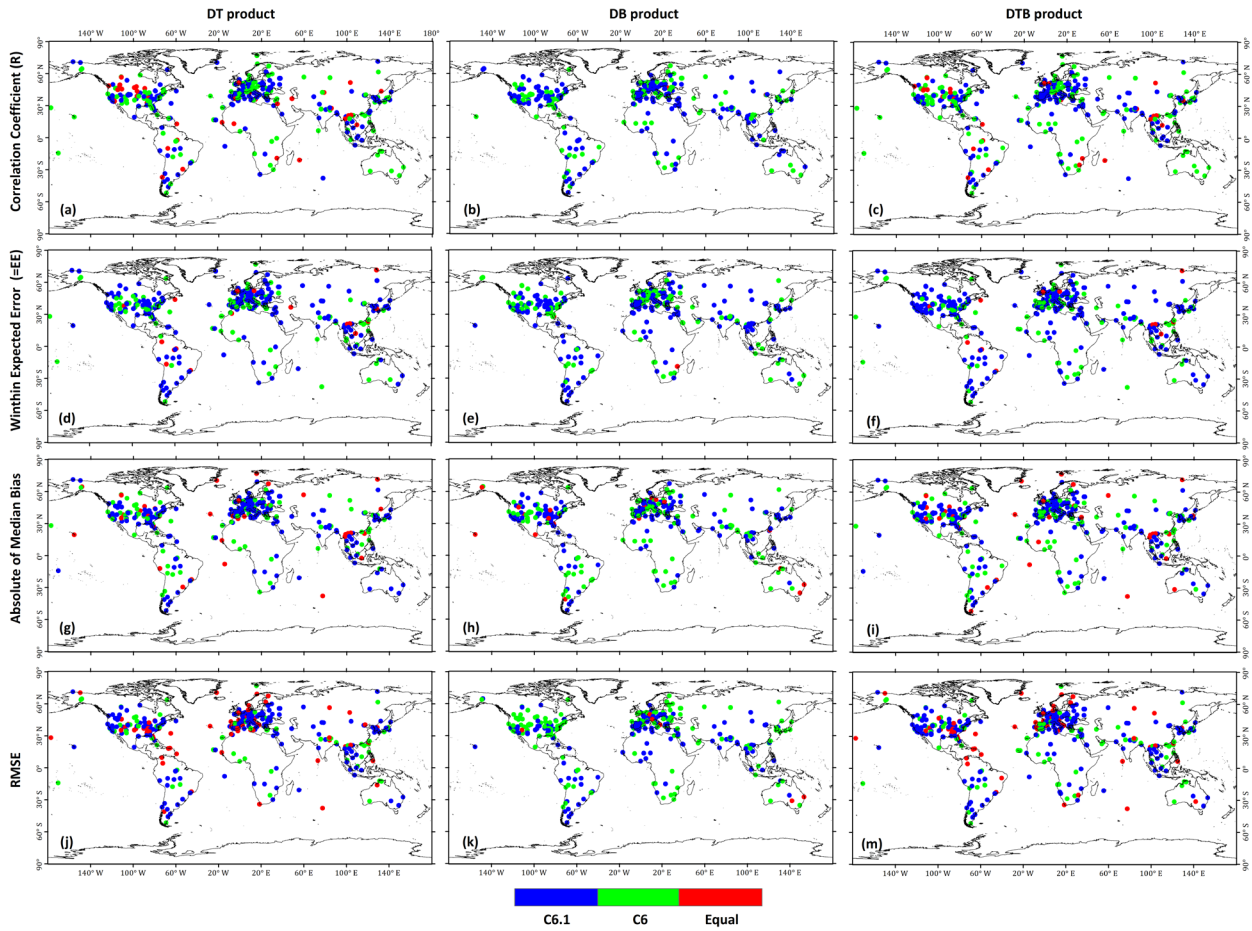
Figure S4. Maps showing the best performance of MODIS DT, DB and DTB algorithms across each site between C6.1 and C6 by different statistical metrics: (a) data collections, (b) percentage of collections falling within the EE, (c) median bias and (d) RMSE
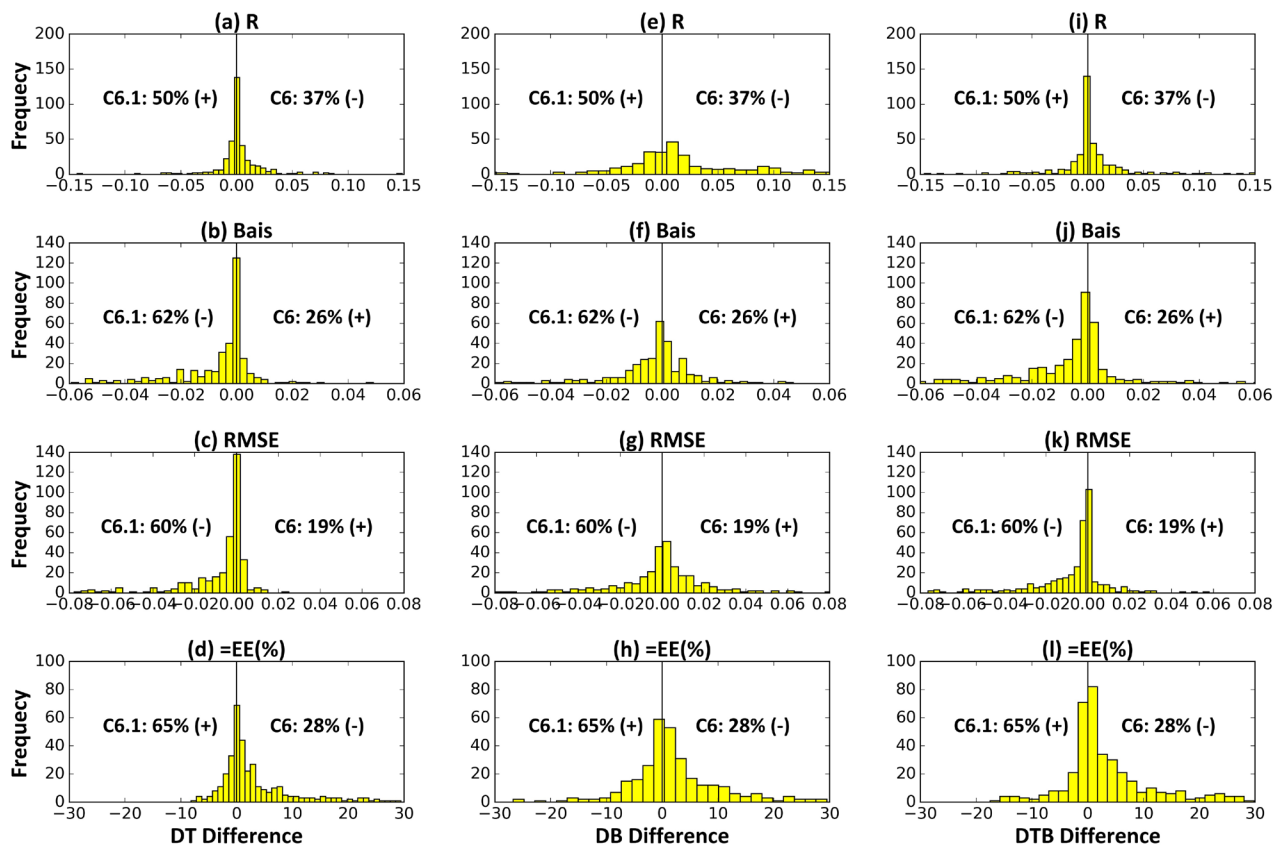
Figure S5. Frequency histograms of (C6.1 DT – C6 DT, a-d), (C6.1 DB – C6 DB, e-h) and (C6.1 DTB – C6 DTB, i-l) differences in validation statistics for the ensemble of sites with at least 20 retrievals. The statistics are the correlation coefficient (R), the absolute value of the median bias, the root-mean-square error (RMSE), and the percentage of retrievals within the EE envelope (=EE, %). For each metric, the fraction of sites where each algorithm performs best is shown in each panel. The annotation represents the proportions for validation statistics, where the plus and minus signs in parentheses indicate the negative and positive values.

(a) Best algorithm by data collections

(b) Best algorithm by fraction within EE

(c) Best algorithm by median bias

(d) Best algorithm by RMSE

DT   DB   DTB   DT=DTB   DB=DTB   DT=DB=DTB

Figure S6. Geographical distribution of sites showing where the MODIS C6 DT, DB, and DTB algorithms performed the best on land according to different statistical metrics: (a) the number of retrievals, (b) the percentage of points falling within the EE envelope, (c) the median bias, and (d) the root-mean-square error (RMSE).
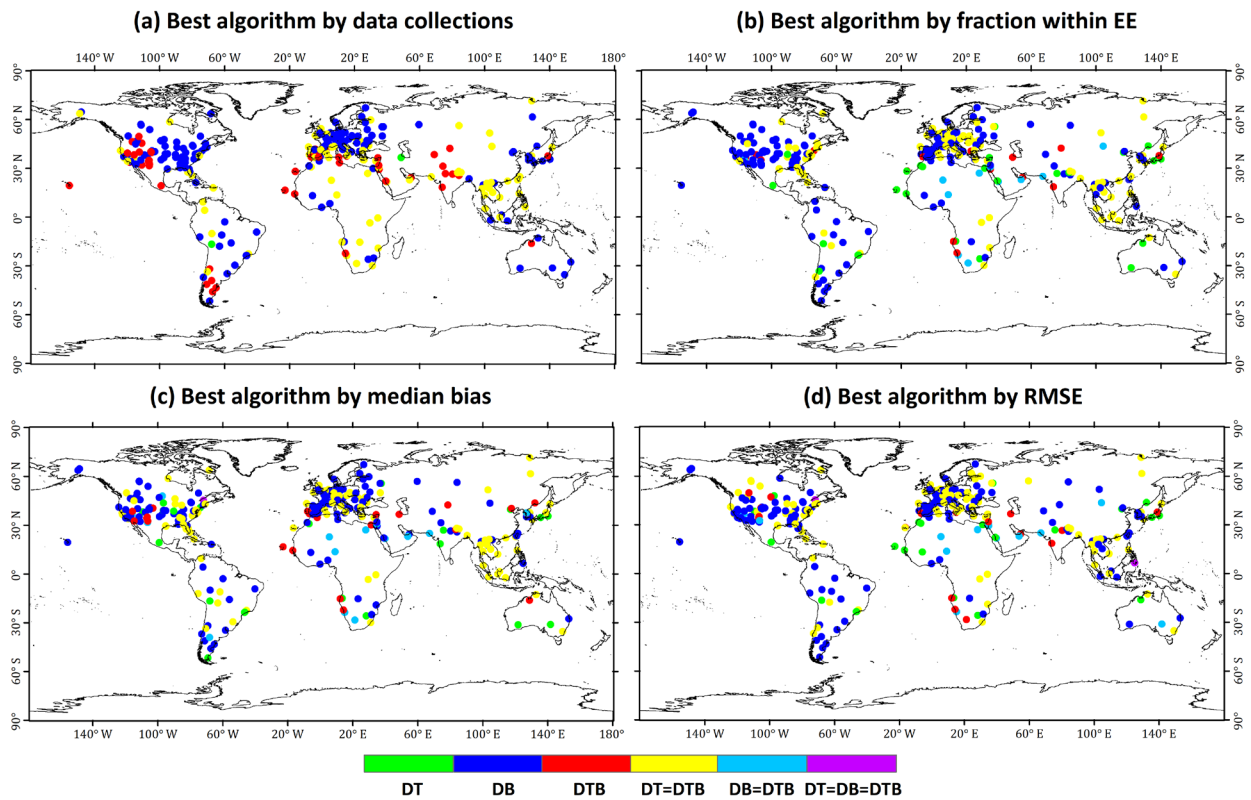
Table S1. Review of related studies on aerosol retrieval algorithms for satellite sensors

Satelite	Full name	Related study
AATSR	Advanced AlongTrack Scanning Radiometer	Veefkind & de Leeuw, 1998; North et al., 1999
AVHRR	Advanced Very High Resolution Radiometer	Li et al., 2013; Riffler et al., 2010
Gaofen	-	She et al., 2017; Sun et al., 2017
GOCI	Geostationary Ocean Color Imager	Choi et al., 2016
HJ-1	Huanjing-1	Sun et al., 2010; Li et al., 2012
Himawari-8	-	Ge et al., 2018; Yan et al., 2018
Landsat	-	Lyapustin, et al., 2003; Wei et al., 2017
MERIS	Medium-resolution imaging spectrometer	Santer et al., 2007; Ramon & Santer, 2001
MISR	Multi-angle Imaging Spectro-Radiometer	Kahn et al., 2010; Martonchik et al., 1997
MODIS	Moderate Resolution Imaging Spectro-radiometer	Kaufman et al., 1997; Levy et al., 2007; Hsu et al., 2004, 2006.
OMI	Ozone Monitoring Instrument	Livingston et al., 2009; Torres et al., 2007
SeaWiFS	Sea-Viewing Wide Field-of-View Sensor	Sayer et al., 2012
TOMS	Total Ozone Mapping Spectrometer	Hsu et al., 1999; Torres et al., 2002
VIIRS	Visible Infrared Imaging Radiometer Suite	Jackson et al., 2013; Liu et al., 2014

Table S2. Statistics of annual mean aerosols for land, ocean and each region calculated from Terra C6.1 and C6 DT, DB and DTB AOD datasets from 2013 to 2017

Algorithm	DT		DB		DTB	
Collection	C6.1	C6	C6.1	C6	C6.1	C6
Ocean	0.162±0.070	0.159±0.070	-	-	0.162±0.070	0.159±0.070
Land	0.220±0.152	0.217±0.148	0.210±0.140	0.207±0.133	0.217±0.142	0.216±0.137
EAA	0.262±0.158	0.252±0.148	0.220±0.130	0.218±0.132	0.239±0.450	0.240±0.136
SAA	0.500±0.184	0.497±0.188	0.356±0.185	0.365±0.181	0.393±0.201	0.404±0.198
SEA	0.310±0.090	0.310±0.091	0.360±0.130	0.312±0.109	0.310±0.090	0.311±0.091
EUR	0.182±0.155	0.177±0.143	0.180±0.051	0.197±0.087	0.180±0.100	0.171±0.098
ENAM	0.157±0.037	0.159±0.037	0.155±0.041	0.157±0.045	0.158±0.037	0.161±0.037
WNAM	0.153±0.042	0.153±0.040	0.107±0.053	0.116±0.054	0.132±0.045	0.140±0.041
SAM	0.162±0.079	0.164±0.080	0.161±0.093	0.153±0.064	0.153±0.079	0.159±0.077
NAME	0.336±0.167	0.337±0.175	0.343±0.125	0.331±0.132	0.340±0.109	0.335±0.117
SAF	0.218±0.160	0.217±0.159	0.187±0.152	0.174±0.103	0.206±0.163	0.212±0.160
OCE	0.093±0.053	0.094±0.053	0.050±0.046	0.061±0.040	0.061±0.051	0.066±0.050

Table S3. Statistics describing the relationships between Terra C6 DT, DB, and DTB AOD retrievals and AERONET AOD measurements for each region from 2013 to 2017.

Region	N			R			MDB			RMSE			Within EE (%)		
	DT	DB	DTB	DT	DB	DTB	DT	DB	DTB	DT	DB	DTB	DT	DB	DTB
EAA	4449	4816	**5738**	0.915	**0.933**	0.931	0.054	**0.010**	0.045	0.171	**0.146**	0.160	59.2	**64.3**	63.0
SAA	2136	2316	**2440**	0.863	0.867	0.860	0.035	-0.083	**0.008**	0.201	0.218	**0.200**	62.1	49.2	**58.9**
SEA	**2246**	1866	**2247**	**0.904**	0.871	**0.904**	0.034	0.014	0.034	0.201	0.196	0.201	**59.4**	49.8	**59.3**
EUR	15494	16143	**16465**	0.845	0.770	0.842	0.039	**-0.009**	0.036	0.086	**0.070**	0.081	67.4	**78.7**	68.7
ENAM	8500	**9020**	8772	**0.916**	0.729	0.901	0.025	**0.015**	0.024	**0.071**	0.072	0.073	77.1	**78.4**	76.2
WNAM	6511	9420	**9638**	0.808	**0.837**	0.801	0.049	**0.007**	0.030	0.122	**0.078**	0.103	55.2	**80.6**	67.4
SAM	3157	3829	3736	0.916	0.925	0.930	0.024	**0.002**	0.013	0.094	**0.059**	0.079	67.5	**84.1**	80.0
NAME	1841	7842	**8208**	0.905	0.802	0.802	0.008	0.023	0.029	0.144	0.175	0.171	64.6	49.4	51.3
SAF	1329	1800	**2035**	0.908	0.823	0.862	-0.009	-0.014	-0.004	0.090	0.094	0.095	75.8	69.6	70.5
OCE	1394	**2365**	2190	0.664	0.461	0.594	0.004	-0.011	0.002	0.049	0.053	0.051	83.5	82.3	82.6

Table S4. Percentage of sites where a given algorithm performed best on land for a given metric. Data are from 2013 to 2017. The metrics are number of retrievals (N), correlation coefficient (R), estimated error (EE), median bias (MDB), and root-mean-square error (RMSE).

Collection	Collection 6.1					Collection 6				
Best in	N	R	EE	|MDB|	RMSE	N	R	EE	|MDB|	RMSE
DT	00.64	16.35	08.01	06.73	07.69	00.32	18.33	06.75	05.14	07.07
DB	**51.92**	24.68	**49.04**	**48.08**	**47.44**	**45.66**	21.86	**53.70**	**52.41**	**52.73**
DTB	17.63	09.94	06.41	07.69	00.00	16.40	08.36	07.40	08.04	00.00
DTB=DT	29.81	**46.15**	33.01	32.69	33.65	37.62	**47.27**	29.26	29.26	27.33
DTB=DB	00.00	02.88	03.53	04.49	04.49	00.00	03.22	02.89	04.18	05.14

References

Choi, M., Kim, J., Lee, J., Kim, M., Park, Y. J., & Jeong, U., et al. (2016). GOCI Yonsei aerosol retrieval (YAER) algorithm and validation during the dragon-ne Asia 2012 campaign. Atmospheric Measurement Techniques, 8(9), 9565-9609.

Ge, B., Li, Z., Liu, L., Yang, L., Chen, X., & Hou, W., et al. (2018). A dark target method for himawari-8/ahi aerosol retrieval: application and validation. IEEE Transactions on Geoscience & Remote Sensing, PP(99), 1-14.

Hsu, N. C., Herman, J. R., Torres, O., Holben, B. N., Tanre, D., & Eck, T. F., et al. (1999). Comparison of the TOMS aerosol index with sun-photometer aerosol optical thickness: results and applications. Journal of Geophysical Research Atmospheres, 104(D6), 6269-6279.

Jackson, J. M., Liu, H., Laszlo, I., Kondragunta, S., Remer, L. A., & Huang, J., et al. (2013). Suomi-NPP VIIRS aerosol algorithms and data products. Journal of Geophysical Research Atmospheres, 118(22), 12-12,689.

Kahn, R. A., Gaitley, B. J., Garay, M. J., Diner, D. J., Eck, T. F., & Smirnov, A., et al. (2010). Multiangle imaging spectroradiometer global aerosol product assessment by comparison with the aerosol robotic network. Journal of Geophysical Research Atmospheres, 115(D23), -.

Li, Y., Xue, Y., de Leeuw, G.D., Li, C., Yang, L., Hou, T., Marir, F., 2013. Retrieval of aerosol optical depth and surface reflectance over land from NOAA AVHRR data. Remote Sensing of Environment. 133, 1-20.

Li, Y., Xue, Y., He, X., & Jie, G. (2012). High-resolution aerosol remote sensing retrieval over urban areas by synergetic use of hj-1 ccd and modis data. Atmospheric Environment, 46(1), 173-180.

Li, Y., Xue, Y., He, X., & Jie, G. (2012). High-resolution aerosol remote sensing retrieval over urban areas by synergetic use of HJ-1 CCD and MODIS data. Atmospheric Environment, 46(1), 173-180.

Lin, S., Sun, C. K., Liu, Q. H., & Bo, Z. (2010). Aerosol optical depth retrieval by hj-1/ccd supported by modis surface reflectance data.Science China Earth Sciences, 53(s1), 74-80.

Liu, H., Remer, L. A., Huang, J., Kondragunta, S., Laszlo, I., & Oo, M., et al. (2014). Preliminary evaluation of S-NPP VIIRS aerosol optical thickness. Journal of Geophysical Research Atmospheres, 119(7), 3942-3962.

Livingston, J. M., Redemann, J., Russell, P. B., & Torres, O. (2009). Comparison of aerosol optical depths from the ozone monitoring instrument (OMI) on aura with results from airborne sunphotometry, other space and ground measurements during milagro/intex-b. Atmospheric Chemistry & Physics, 9(2), págs. 537-540.

Lyapustin, A., Williams, D. L., Markham, B., Irons, J., Holben, B., & Wang, Y. (2003). A method for unbiased high-resolution aerosol retrieval from landsat. Journal of the Atmospheric Sciences, 61(11), 1233-1244.

Martonchik, J. V., Diner, D. J., Kahn, R. A., Ackerman, T. P., Verstraete, M. M., & Pinty, B., et al. (1997). Techniques for the retrieval of aerosol properties over land and ocean using multi-angle imaging. IEEE Transactions on Geoscience & Remote Sensing, 36(4), 1212-1227.

North, P. R. J., Briggs, S. A., Plummer, S. E., and Settle, J. J. (1999) Retrieval of land surface bidirectional reflectance and aerosol opacity from ATSR-2 multi-angle imagery, IEEE T. Geosci. Remote, 37, 526–537.

Ramon, D. and Santer, R. (2001). Operational remote sensing of aerosols over land to account for directional effects, Appl. Optics, 40, 3060–3075.

Riffler, M., Popp, C., Hauser, A., Fontana, F., Wunderle, S., 2010. Validation of a modified AVHRR aerosol optical depth retrieval algorithm over Central Europe. Atmos. Meas. Tech. 3, 1255–1270.

Santer, R., Ramon, D., Vidot, J., and Dilligeard, E. (2007). A Surface Reflectance Model for Aerosol Remote Sensing over Land, Int. J. Remote Sens., 28, 737–760.

Sayer, A. M., Hsu, N. C., Bettenhausen, C., Ahmad, Z., Holben, B. N., & Smirnov, A., et al. (2012). SeaWiFS ocean aerosol retrieval (SOAR): algorithm, validation, and comparison with other data sets. Journal of Geophysical Research Atmospheres, 117(D3), -.

Sayer, A. M., Hsu, N. C., Lee, J., Bettenhausen, C., Kim, W. V., & Smirnov, A. (2017). Satellite ocean aerosol retrieval (SOAR) algorithm extension to S-NPP VIIRS as part of the 'deep blue' aerosol project. Journal of Geophysical Research Atmospheres, 123(1).

She, L., Mei, L., Xue, Y., Che, Y., & Guang, J. (2017). Sahara: a simplified atmospheric correction algorithm for chinese gaofen data: 1. aerosol algorithm. Remote Sensing, 9(3), 253.

Sun L., Sun, C. K., Liu, Q. H., & Bo, Z. (2010). Aerosol optical depth retrieval by HJ-1/CCD supported by MODIS surface reflectance data. Science China Earth Sciences, 53(S1), 74-80.

Sun, K., Chen, X., Zhu, Z., & Zhang, T. (2017). High resolution aerosol optical depth retrieval using gaofen-1 wfv camera data. Remote Sensing,9(1), 89.

Torres, O., Bhartia, P.K., Herman, J.R., Sinyuk, A., Ginoux, P., Holben, B., 2002. A long-term record of aerosol optical depth from TOMS observations and comparison to AERONET measurements. J. Atmos. Sci. 59, 398–413.

Torres, O., Tanskanen, A., Veihelmann, B., Ahn, C., Braak, R., Bhartia, P.K., Veefkind, P., Levelt, P., 2007. Aerosols and surface UV products from Ozone monitoring instrument observations: an overview. Journal of Geophysical Research, 112, D24S47.

Veefkind, J. P. and de Leeuw, G. (1998). A new algorithm to determine the spectral aerosol optical depth from satellite radiometer measurements, J. Aerosol Sci. 29, 1237–1248.

Wei, J., Huang, B., Sun, L., Zhang, Z., Wang, L., & Bilal, M. (2017). A simple and universal aerosol retrieval algorithm for landsat series images over complex surfaces. Journal of Geophysical Research Atmospheres,122(24).

Yan, X., Li, Z., Luo, N., Shi, W., Zhao, W., & Yang, X., et al. (2018). A minimum albedo aerosol retrieval method for the new-generation geostationary meteorological satellite Himawari-8. Atmospheric Research, 207.